TECHNICAL ARTICLE

Crystal structure of salmeterol xinafoate form I (Serevent®Diskus®), $(C_{25}H_{37}NO_4)(C_{11}H_8O_3)$

James A. Kaduk,[1,a] Kai Zhong,[2] Amy M. Gindhart,[2] and Thomas N. Blanton[2]
[1]*Illinois Institute of Technology, 3101 S. Dearborn St., Chicago, Illinois 60616*
[2]*ICDD, 12 Campus Blvd., Newtown Square, Pennsylvania 19073-3273*

(Received 14 May 2015; accepted 27 September 2015)

The crystal structure of salmeterol xinafoate has been solved and refined using synchrotron X-ray powder diffraction data, and optimized using density functional techniques. Salmeterol xinafoate crystallizes in space group $P\bar{1}$ (#2) with $a = 9.173\,89(13)$, $b = 9.483\,79(14)$, $c = 21.3666(4)$ Å, $\alpha = 82.2646(13)$, $\beta = 85.2531(12)$, $\gamma = 62.1565(11)°$, $V = 1628.37(5)$ Å^3, and $Z = 2$. Key to the structure solution was linking the two fragments by a Li atom along the expected N–H···O hydrogen bond. The salmeterol cation and xinafoate anion are linked by N–H···O and O–H···O hydrogen bonds, interactions which cause the salmeterol to adjust its conformation. The hydrogen bonds result in complex chains along the *b*-axis. The powder pattern is included in the Powder Diffraction File™ as entry 00-065-1430. © *2015 International Centre for Diffraction Data*. [doi:10.1017/S0885715615000743]

Key words: salmeterol xinafoate, Serevent Diskus, powder diffraction, Rietveld refinement, density functional theory

I. INTRODUCTION

Salmeterol xinafoate is a long-acting β_2-adrenergic receptor agonist drug used for the treatment of asthma and chronic obstructive pulmonary disease. It is the active ingredient in Serevent®. Generation of two crystalline polymorphic forms using solution-enhanced dispersion by supercritical fluids has been reported (Beach *et al*., 1999). Form I is the stable polymorph under ambient conditions and the main phase in commercial material. Form II is the metastable form. The systematic name (CAS Registry Number 94 749-08-3) is 4-hydroxy-α^1-[[[6-(4-phenylbutoxy)hexyl]amino]methyl]-1,3-benzenedimethanol 1-hydroxy-2-naphthalenecarboxylate, and a two-dimensional molecular diagram is shown in Figure 1.

The presence of high-quality reference powder patterns in the Powder Diffraction File (PDF™; ICDD, 2014) is important for phase identification, particularly by pharmaceutical, forensic, and law enforcement scientists. The crystal structures of a significant fraction of the largest dollar volume pharmaceuticals have not been published, and thus calculated powder patterns are not present in the PDF-4 databases. Sometimes experimental patterns are reported, but they are generally of low quality. This structure is a result of a collaboration among International Centre for Diffraction Data (ICDD), Illinois Institute of Technology (IIT), Poly Crystallography Inc., and Argonne National Laboratory to measure high-quality synchrotron powder patterns of commercial pharmaceutical ingredients, include these reference patterns in the PDF, and determine the crystal structures of these active pharmaceutical ingredients (APIs).

Even when the crystal structure of an API is reported, the single-crystal structure was often determined at low temperature. Most powder diffraction measurements are performed at ambient conditions. Thermal expansion (generally anisotropic) means that the peak positions calculated from a low-temperature single-crystal structure often differ significantly from those measured at ambient conditions, even if the structure remains the same. These peak shifts can result in failure of default search/match algorithms to identify a phase, even when it is present in the sample. High-quality reference patterns measured at ambient conditions are thus critical for easy identification of APIs using standard powder diffraction practices.

II. EXPERIMENTAL

Salmeterol xinafoate was a commercial reagent (>97% purity), purchased from Key Organics Limited (batch 74 745), and was used as-received. The white powder was packed into a 1.5 mm diameter Kapton capillary and rotated during the measurement at ~50 cycles s^{-1}. The powder diffraction pattern was measured at 295 K at beam line 11-BM (Lee *et al*., 2008; Wang *et al*., 2008) of the Advanced Photon Source at Argonne National Laboratory using a wavelength of 0.413 891 Å from 0.5°2θ to 50°2θ with a step size of 0.001° and a counting time of 0.1 s step^{-1}. The pattern was indexed on a primitive triclinic unit cell having $a = 9.174$, $b = 9.481$, $c = 21.732$ Å, $\alpha = 82.3$, $\beta = 85.2$, $\gamma = 62.2°$, $V = 1628.3$ Å^3, and $Z = 2$ using Jade 9.5 (MDI, 2014). Assuming $Z = 2$ yields an atomic volume of 18.5 Å^3 atom^{-1} for the 88 non-H atoms in the unit cell, and a reasonable calculated density of 1.225 g cm^{-3}. Since commercial material is a racemate, the space group was assumed to be $P\bar{1}$ (#2), which was confirmed by successful solution and refinement of the structure. A reduced cell search in the Cambridge Structural Database

[a]Author to whom correspondence should be addressed. Electronic mail: kaduk@polycrystallography.com

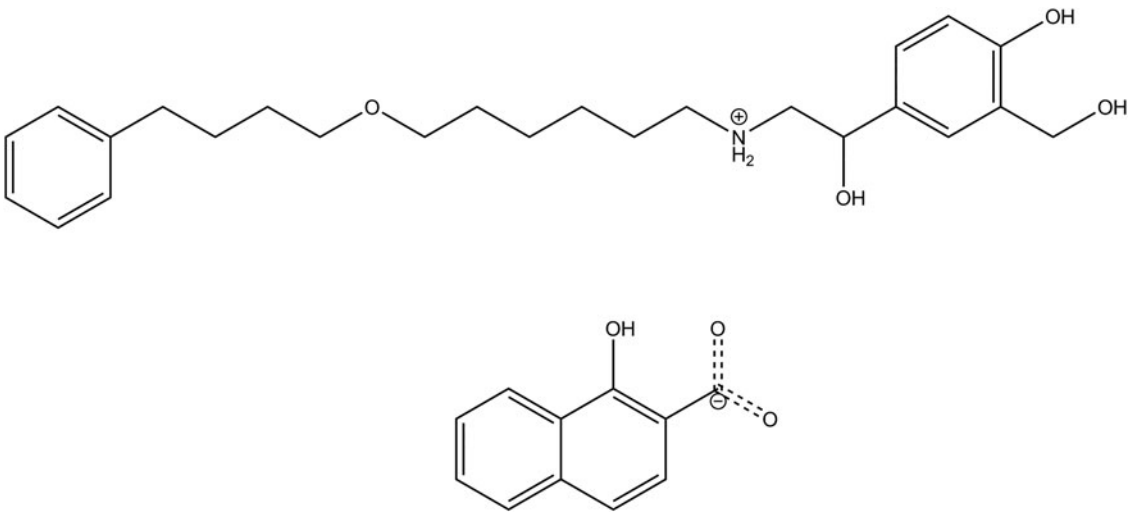

Figure 1. The molecular structure of salmeterol xinafoate.

(Allen, 2002) combined with the chemistry "C H N O only" yielded 48 hits, but no structure for salmeterol xinafoate. A name search on "salmeterol" yielded no hits, as did a connectivity search on a salmeterol molecule.

A salmeterol cation and a xinafoate anion were built and their conformations optimized using Spartan '14 (Wavefunction, 2013), and saved as mol2 files. Manual intervention was needed to keep the alkyl chains in all-*trans* conformations. These files were converted into Fenske–Hall *Z*-matrix files using OpenBabel (O'Boyle *et al.*, 2011). Many attempts to solve the structure with FOX (Favre-Nicolin and Černý, 2002) and DASH (David *et al.*, 2006) using these two fragments yielded solutions with molecular overlap and voids. Some contained linear salmeterol and others yielded bent conformations. Direct methods using EXPO2013 (Altomare *et al.*, 2013) suggested relatively linear arrays of atoms, but did not yield enough of the structure to permit manual completion.

It would be very surprising if the positively-charged NH_2 group of the salmeterol cation and the ionized carboxylate group of the xinafoate anion did not participate in strong N–H···O hydrogen bonds. Accordingly, the salmeterol and xinafoate fragments were oriented so that the N···O distance was 2.80 Å and a hydrogen bond was linear. This was done for both carboxylate oxygens and both N–H hydrogens, and one arrangement of the four yielded a much better fit to the pattern. The N–H hydrogen was removed, and replaced by a Li atom at the midpoint of the N···O vector, to tie the two fragments into one. This "superfragment" was used to solve the structure with FOX. The maximum $\sin\theta/\lambda$ used in the solution was 0.25 $Å^{-1}$ (d_{min} = 2.00 Å). Because the predicted morphology of most trial models was platy, with {001} as the principal faces, a March–Dollase preferred orientation model (unique axis = 001) was included in the structure solution.

Rietveld refinement was carried out using General Structure Analysis System (GSAS) (Toby, 2001; Larson and Von Dreele, 2004). Only the 1.0–20.0° portion of the pattern was included in the refinement (d_{min} = 1.19 Å). All non-H bond distances and angles were subjected to restraints, based on a Mercury/Mogul Geometry Check (Bruno *et al.*, 2004; Sykes *et al.*, 2011) of the molecule. The Mogul average and standard deviation for each quantity were used as the restraint parameters. Planar restraints were applied to the two benzene rings and the naphthalene ring system. The restraints contributed 4.88% to the final χ^2. Isotropic displacement coefficients were refined, grouped by chemical similarity. The hydrogen atoms were included in calculated positions, which were recalculated during the refinement using Materials Studio (Accelrys, 2013). The U_{iso} of each hydrogen atom was constraint to be 1.3× that of the heavy atom to which it is attached. The peak profiles were described using profile function #4 (Thompson *et al.*, 1987; Finger *et al.*, 1994), which includes the Stephens (1999) anisotropic strain broadening model. The background was modeled using a 3-term shifted Chebyshev polynomial, with a 4-term diffuse scattering function to model the Kapton capillary and any amorphous component. The refinement yielded the residuals R_{wp} = 0.1199, R_p = 0.1011, and χ^2 = 2.822. Re-starting the Rietveld refinement from the density functional theory (DFT)-optimized model led to a model yielding lower residuals (R_{wp} = 0.1075 and χ^2 = 2.296), but with a different chain conformation at C21–C24, a different orientation of the hydroxymethyl group C7–O8, and a slightly different conformation around N13. A new DFT calculation indicated that this model was 49 kcal $mole^{-1}$ lower in energy than the first model. The final refinement was started from this second DFT model.

The final refinement of 165 variables using 19 116 observations (18 999 data points and 117 restraints) yielded the residuals R_{wp} = 0.1035, R_p = 0.0873, and χ^2 = 2.120. The largest peak (0.21 Å from N13) and hole (1.19 Å from O44) in the difference Fourier map were 0.26 and −0.24 $eÅ^{-3}$, respectively. The Rietveld plot is included as Figure 2. The largest errors are in the shapes of the low-angle peaks (particularly the strong 001 peak), and may indicate subtle changes in the sample during the measurement.

A density functional geometry optimization (fixed experimental unit cell) was carried out using CRYSTAL14 (Dovesi *et al.*, 2014). The basis sets for the H, C, N, and O atoms were those of Gatti *et al.* (1994). The calculation was run on eight 2.1 GHz Xeon cores (each with 6 Gb RAM) of a 304-core Dell Linux cluster at IIT, used eight *k*-points and the B3LYP functional, and took ∼32 h.

https://doi.org/10.1017/S0885715615000743 Published online by Cambridge University Press

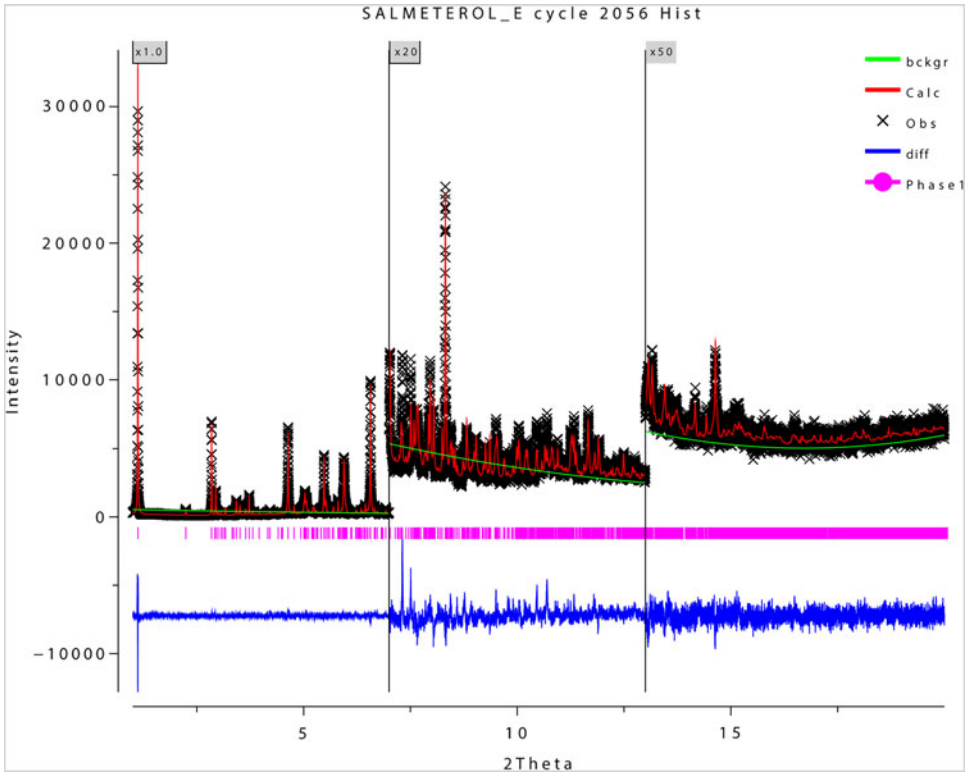

Figure 2. (Colour online) The Rietveld plot for the refinement of salmeterol xinafoate. The black crosses represent the observed data points, and the red line is the calculated pattern. The blue curve is the difference pattern, plotted at the same vertical scale as the other patterns, and the green line is the background. The vertical scale has been multiplied by a factor of 20 for $2\theta > 7.0°$, and by a factor of 50 for $2\theta > 13.0°$.

III. RESULTS AND DISCUSSION

The powder pattern corresponds to that of salmeterol xinafoate Form I (Beach *et al*., 1999; Tong *et al*., 2001), the stable form at ambient conditions. The refined atom coordinates of salmeterol xinafoate are reported in Table I, and the coordinates from the DFT optimization in Table II. The root-mean-square deviation of the non-H atoms in the salmeterol cation is 0.256 Å (Figure 3). This good agreement between the refined and optimized structures is strong evidence that the experimental structure is correct (van de Streek and Neumann, 2014). The largest differences are in the conformation of the C22–C24 chain carbon atoms. The discussion of the geometry uses the DFT-optimized structure. The asymmetric unit (with atom numbering) is illustrated in Figure 4, and the crystal structure is presented in Figure 5. The large displacement coefficients of the atoms in the C25–C30 phenyl ring presumably reflect disorder in this portion of the molecule. We felt that detailed modeling of the disorder was beyond the scope of this study.

All of the bond distances fall within the normal ranges indicated by a Mercury Mogul Geometry check (Macrae *et al.*, 2008). The C6–C5–C10 angle of 125.0° is flagged as unusual [average = 120.0(16)°; Z-score = 3.1]. The hydroxyl group O11 participates in a strong hydrogen bond to the carboxylate group of the xinafoate, so the unusual geometry can be rationalized. Similarly, the torsion angles C12–C10–C5–C4 and C12–C10–C5–C6 are unusual; the hydrogen bonds involving O11 seem to have resulted in distortions of that region of the molecule.

A semi-empirical conformation examination (RHF/PM3) using Spartan '14 (Wavefunction, 2013) indicated that the observed conformation of the salmeterol cation is ~27 kcal mole^{-1} higher in energy than a local minimum. A molecular mechanics force field (MMFF) sampling of conformational space indicated that the optimized solid state conformation is 19 kcal mole^{-1} higher in energy than the minimum energy conformation, which folded on itself to form a compact molecule. The energy difference indicates that hydrogen bonds and van der Waals forces contribute significantly to the crystal energy and to the extended salmeterol conformation observed in the solid state.

Analysis of the contributions to the total crystal energy using the Forcite module of Materials Studio (Accelrys, 2013) suggests that the intramolecular deformation energy contains about equal contributions from bond angle and torsion angle distortion terms. The intermolecular energy is dominated by electrostatic contributions, which in this force–field-based analysis include hydrogen bonds. The hydrogen bonds are better analyzed using the results of the DFT calculation.

As expected, there is a strong N13–H56···O43 hydrogen bond between the cationic portion of the salmeterol and the ionized carboxylate of the xinafoate (Table III). This is a discrete hydrogen bond, with graph set *D*1,1(2) (Etter, 1990; Bernstein *et al.*, 1995; Shields *et al.*, 2000). The other hydrogen atom of the cation forms an even stronger N13–H89···O8 hydrogen bond to the hydroxymethyl oxygen O8; this hydrogen bond participates in patterns with graph sets *R*2,2(18), *C*2,2(11) and larger patterns. The hydroxyl groups O9 and O11 make *D1,1(2)* hydrogen bonds to the ionized carboxylate, and the hydroxyl group O8 participates in *R*2,2(32) and larger hydrogen bond patterns. There is an intramolecular

https://doi.org/10.1017/S0885715615000743 Published online by Cambridge University Press

TABLE I. Rietveld refined crystal structure of salmeterol xinafoate Form I.

Crystal data	
$C_{36}H_{45}NO_7$	$\beta = 85.2531(12)°$
$M_r = 603.76$	$\gamma = 62.1565(11)°$
Triclinic, $P\bar{1}$ (#2)	$V = 1628.37(3)$ Å^3
$a = 9.173\,89(13)$ Å	$Z = 2$
$b = 9.483\,79(14)$ Å	Synchrotron radiation, $\lambda = 0.413\,891$ Å
$c = 21.3666(4)$ Å	$T = 295$ K
$\alpha = 82.2646(13)°$	Cylinder, 1.5×1.5 mm^2
Data collection	
11-BM APS diffractometer	Scan method: step
Specimen mounting: Kapton capillary	$2\theta_{min} = 0.5°$, $2\theta_{max} = 50.0°$, $2\theta_{step} = 0.001°$
Data collection mode: transmission	
Refinement	
Least-squares matrix: full	18 999 data points
$R_p = 0.087$	Profile function: CW Profile function number 4 with 27 terms Pseudovoigt profile coefficients as parameterized in Thompson *et al.* (1987). Asymmetry correction of Finger *et al.* (1994). Microstrain broadening by Stephens (1999). #1 (GU) = 1.163 #2(GV) = −0.126 #3(GW) = 0.063 #4(GP) = 0.000 #5(LX) = 0.173 #6(ptec) = 0.00 #7(trns) = 0.00 #8(shft) = −0.1346 #9 (sfec) = 0.00 #10(S/L) = 0.0011 #11(H/L) = 0.0011 #12(eta) = 1.0000 Peak tails are ignored where the intensity is below 0.0020 times the peak Aniso. broadening axis 0.0 0.0 1.0
$R_{wp} = 0.104$	165 parameters
$R_{exp} = 0.073$	117 restraints
$R(F^2) = 0.109\,41$	$(\Delta/\sigma)_{max} = 0.13$
$\chi^2 = 2.132$	Background function: GSAS Background function number 1 with 3 terms. Shifted Chebyshev function of 1st kind 1: 249.2842: −209.4443: 79.9333

Fractional atomic coordinates and isotropic displacement parameters (Å^2).

	x	*y*	*z*	U_{iso}
C1	−0.5603(4)	0.6467(6)	0.6262(3)	0.083(3)
C2	−0.6638(4)	0.8113(6)	0.6179(3)	0.083(3)
C3	−0.6464(4)	0.9043(6)	0.5647(4)	0.083(3)
C4	−0.5252(4)	0.8333(8)	0.5195(3)	0.083(3)
C5	−0.4203(4)	0.6695(8)	0.5266(3)	0.083(3)
C6	−0.4390(4)	0.5778(6)	0.5800(3)	0.083(3)
C7	−0.5981(14)	0.5433(11)	0.6774(4)	0.083(3)
O8	−0.7245(16)	0.5182(15)	0.6604(6)	0.083(3)
O9	−0.7628(16)	0.8861(11)	0.6683(4)	0.083(3)
C10	−0.2835(10)	0.5953(11)	0.4783(3)	0.0310(16)
O11	−0.1673(12)	0.6547(12)	0.4773(5)	0.0310(16)
C12	−0.191(2)	0.4149(11)	0.4883(5)	0.0310(16)
N13	−0.0768(19)	0.3555(9)	0.4343(5)	0.0310(16)
C14	0.032(2)	0.1842(11)	0.4399(5)	0.0310(16)
C15	0.107(3)	0.1368(12)	0.3751(5)	0.0310(16)
C16	0.2222(16)	−0.0367(14)	0.3707(5)	0.0310(16)
C17	0.3236(16)	−0.0748(18)	0.3091(5)	0.0310(16)
C18	0.4649(17)	−0.0339(19)	0.3069(5)	0.0310(16)
C19	0.5817(17)	−0.0833(12)	0.2507(6)	0.0310(16)
O20	0.6437(15)	−0.2481(12)	0.2431(5)	0.0310(16)
C21	0.7624(6)	−0.2922(12)	0.1930(4)	0.0310(16)
C22	0.7915(13)	−0.4477(17)	0.1717(7)	0.0310(16)
C23	0.9638(13)	−0.5262(10)	0.1490(5)	0.0310(16)
C24	1.0348(17)	−0.7008(8)	0.1495(4)	0.0310(16)
C25	1.0934(11)	−0.7559(5)	0.0879(3)	0.1996)
C26	0.9980(10)	−0.7910(6)	0.0527(4)	0.199(6)
C27	1.0529(16)	−0.8433(9)	−0.0057(4)	0.199(6)
C28	1.2043(18)	−0.8610(7)	−0.0293(4)	0.199(6)
C29	1.2999(10)	−0.8263(5)	0.0054(6)	0.199(6)
C30	1.2448(10)	−0.7739(7)	0.0639(5)	0.199(6)
C31	0.2187(9)	0.5484(5)	0.2488(3)	0.0656(18)
C32	0.0897(3)	0.6837(6)	0.2710(2)	0.0656(18)
C33	0.0569(3)	0.8343(6)	0.2399(2)	0.0656(18)
C34	0.1389(3)	0.8490(5)	0.1851(3)	0.0656(18)
C35	0.3453(3)	0.7247(7)	0.1019(3)	0.0656(18)
C36	0.4610(3)	0.5909(9)	0.0769(2)	0.0656(18)
C37	0.4960(4)	0.4408(7)	0.1066(3)	0.0656(18)
C38	0.4155(4)	0.4244(5)	0.1610(3)	0.0656(18)
C39	0.2944(3)	0.5597(5)	0.1887(2)	0.0656(18)
C40	0.2593(3)	0.7129(5)	0.1581(2)	0.0656(18)
C41	0.0266(11)	0.6751(8)	0.3371(3)	0.0656(18)
O42	−0.0843(15)	0.7970(9)	0.3592(4)	0.0656(18)
O43	0.0603(18)	0.5350(9)	0.3606(4)	0.0656(18)
O44	0.2589(16)	0.3980(8)	0.2776(4)	0.0656(18)
H45	−0.732 17	1.038 93	0.558 25	0.107(4)
H46	−0.511 06	0.9103	0.475 72	0.107(4)
H47	−0.353 64	0.443 16	0.586 44	0.107(4)
H48	−0.633 26	0.604 54	0.7227	0.107(4)
H49	−0.480 57	0.422 81	0.686 46	0.107(4)
H50	−0.684 88	0.405 66	0.693 62	0.107(4)
H51	−0.837 01	1.0254	0.654 96	0.107(4)
H52	−0.339 45	0.633 32	0.429 42	0.040(2)
H53	−0.147 91	0.694 83	0.433 59	0.040(2)
H54	−0.283 33	0.365 53	0.487 95	0.040(2)
H55	−0.1258	0.374 68	0.534 55	0.040(2)
H56	−0.007 19	0.411 68	0.428 42	0.040(2)
H57	−0.047 63	0.122 36	0.458 43	0.040(2)
H58	0.137 05	0.145 65	0.472 79	0.040(2)
H59	0.161 53	0.211 44	0.352 48	0.040(2)
H60	−0.007 93	0.162 48	0.343 26	0.040(2)
H61	0.160 79	−0.114 52	0.380 68	0.040(2)
H62	0.315 41	−0.069 52	0.4113	0.040(2)
H63	0.237 03	−0.004 85	0.268 58	0.040(2)
H64	0.372 18	−0.209 75	0.306 16	0.040(2)
H65	0.545 16	−0.101 77	0.348 05	0.040(2)
H66	0.410 45	0.098 54	0.307 45	0.040(2)
H67	0.669 21	−0.041 56	0.247 35	0.040(2)
H68	0.490 97	−0.019 12	0.204 07	0.040(2)
H69	0.886 38	−0.3022	0.209 76	0.040(2)
H70	0.716 03	−0.1876	0.153 18	0.040(2)
H71	0.764 35	−0.518 45	0.210 69	0.040(2)
H72	0.711 71	−0.413 93	0.128 97	0.040(2)
H73	0.985 85	−0.466 54	0.104 11	0.040(2)
H74	1.043 08	−0.5048	0.188 15	0.040(2)
H75	0.934 21	−0.733 92	0.167 74	0.040(2)
H76	1.140 88	−0.762 14	0.185 32	0.040(2)
H77	0.871 36	−0.774 17	0.0746	0.259(7)
H78	0.969 72	−0.8704	−0.032 09	0.259(7)
H79	1.244 86	−0.902 48	−0.076 39	0.259(7)
H80	1.421 74	−0.838 34	−0.014	0.259(7)
H81	1.324 17	−0.741 66	0.092 73	0.259(7)
H82	−0.040 34	0.9485	0.259 77	0.085(2)
H83	0.109 32	0.972 75	0.159 96	0.085(2)
H84	0.315 96	0.8473	0.076 81	0.085(2)
H85	0.529 09	0.600 99	0.0314	0.085(2)
H86	0.593 22	0.3278	0.0862	0.085(2)
H87	0.445 54	0.299 07	0.186 34	0.085(2)
H88	0.191 13	0.407 29	0.312 14	0.085(2)
H89	−0.156 52	0.403 78	0.393 73	0.040(2)

https://doi.org/10.1017/S0885715615000743 Published online by Cambridge University Press

TABLE II. DFT-optimized (CRYSTAL09) crystal structure of salmeterol xinafoate Form I.

Crystal data	
$(C_{25}H_{37}NO_4)$	$\beta = 85.2507°$
$(C_{11}H_8O_3)$	
$M_r = 599.77$	$\gamma = 62.1542°$
Triclinic, $P\bar{1}$	$V = 1628.37$ Å^3
$a = 9.1733$ Å	$Z = 2$
$b = 9.4839$ Å	
$c = 21.3679$ Å	
$\alpha = 82.2613°$	

Fractional atomic coordinates and isotropic displacement parameters (Å^2).

	x	y	z	U_{iso}
C1	−0.568 66	0.666 34	0.629 87	0.082 60
C2	−0.668 91	0.833 27	0.620 43	0.082 60
C3	−0.648 45	0.919 46	0.564 58	0.082 60
C4	−0.528 83	0.840 50	0.519 95	0.082 60
C5	−0.422 92	0.675 74	0.529 47	0.082 60
C6	−0.445 78	0.591 15	0.584 79	0.082 60
C7	−0.598 84	0.566 31	0.684 92	0.082 60
O8	−0.690 28	0.494 71	0.662 73	0.082 60
O9	−0.785 51	0.906 52	0.664 71	0.082 60
C10	−0.290 65	0.603 46	0.479 39	0.031 00
O11	−0.176 48	0.667 85	0.477 51	0.031 00
C12	−0.198 65	0.420 15	0.489 52	0.031 00
N13	−0.085 64	0.360 02	0.434 42	0.031 00
C14	0.012 72	0.181 82	0.437 21	0.031 00
C15	0.126 72	0.137 45	0.379 20	0.031 00
C16	0.217 07	−0.043 34	0.374 24	0.031 00
C17	0.331 76	−0.086 02	0.315 71	0.031 00
C18	0.471 92	−0.040 48	0.314 24	0.031 00
C19	0.577 44	−0.076 81	0.254 19	0.031 00
O20	0.659 92	−0.245 67	0.250 17	0.031 00
C21	0.741 72	−0.286 65	0.190 71	0.031 00
C22	0.839 02	−0.467 68	0.193 12	0.031 00
C23	0.932 33	−0.523 35	0.131 35	0.031 00
C24	1.032 17	−0.707 12	0.137 24	0.031 00
C25	1.103 96	−0.770 08	0.074 81	0.198 90
C26	1.014 86	−0.809 84	0.036 51	0.198 90
C27	1.079 52	−0.867 84	−0.021 46	0.198 90
C28	1.235 25	−0.886 80	−0.041 93	0.198 90
C29	1.322 80	−0.841 97	−0.005 32	0.198 90
C30	1.258 03	−0.784 88	0.052 74	0.198 90
C31	0.217 82	0.537 57	0.243 65	0.065 60
C32	0.099 75	0.674 65	0.270 49	0.065 60
C33	0.058 97	0.828 18	0.237 12	0.065 60
C34	0.134 15	0.845 52	0.180 43	0.065 60
C35	0.345 21	0.721 34	0.096 53	0.065 60
C36	0.468 01	0.586 27	0.072 66	0.065 60
C37	0.509 58	0.431 96	0.104 47	0.065 60
C38	0.427 37	0.415 38	0.159 76	0.065 60
C39	0.301 27	0.552 57	0.185 32	0.065 60
C40	0.259 01	0.708 57	0.153 61	0.065 60
C41	0.022 70	0.655 31	0.333 33	0.065 60
O42	−0.080 08	0.775 86	0.360 60	0.065 60
O43	0.067 64	0.511 73	0.358 91	0.065 60
O44	0.259 00	0.388 82	0.271 12	0.065 60
H45	−0.724 94	1.048 06	0.556 59	0.107 40
H46	−0.515 31	0.908 67	0.476 99	0.107 40
H47	−0.367 94	0.462 82	0.594 39	0.107 40
H48	−0.667 76	0.640 64	0.722 54	0.107 40
H49	−0.481 80	0.471 31	0.703 78	0.107 40
H50	−0.684 88	0.405 66	0.693 62	0.107 40
H51	−0.837 01	1.025 40	0.654 96	0.107 40
H52	−0.350 52	0.636 85	0.433 55	0.040 30
H53	−0.147 91	0.694 83	0.433 59	0.040 30
H54	−0.284 72	0.369 66	0.492 48	0.040 30
H55	−0.124 70	0.378 52	0.531 83	0.040 30
H56	−0.007 19	0.411 68	0.428 42	0.040 30
H57	−0.074 91	0.133 34	0.439 66	0.040 30
H58	0.082 10	0.140 47	0.480 71	0.040 30
H59	0.215 53	0.183 31	0.381 20	0.040 30
H60	0.054 32	0.198 39	0.336 61	0.040 30
H61	0.126 11	−0.086 93	0.372 19	0.040 30
H62	0.288 22	−0.106 02	0.417 01	0.040 30
H63	0.258 22	−0.027 19	0.273 21	0.040 30
H64	0.384 54	−0.214 94	0.312 77	0.040 30
H65	0.551 94	−0.102 96	0.354 84	0.040 30
H66	0.423 29	0.088 10	0.317 09	0.040 30
H67	0.669 07	−0.032 74	0.253 47	0.040 30
H68	0.499 35	−0.016 54	0.212 60	0.040 30
H69	0.824 08	−0.231 31	0.180 30	0.040 30
H70	0.649 25	−0.238 91	0.153 62	0.040 30
H71	0.753 55	−0.519 08	0.203 31	0.040 30
H72	0.925 22	−0.513 13	0.232 18	0.040 30
H73	1.015 28	−0.469 84	0.118 24	0.040 30
H74	0.845 24	−0.482 86	0.092 79	0.040 30
H75	0.950 84	−0.758 46	0.157 11	0.040 30
H76	1.130 20	−0.745 31	0.171 32	0.040 30
H77	0.893 98	−0.796 52	0.052 62	0.258 50
H78	1.008 93	−0.898 66	−0.050 24	0.258 50
H79	1.287 72	−0.935 23	−0.086 26	0.258 50
H80	1.442 61	−0.854 01	−0.021 67	0.258 50
H81	1.327 00	−0.751 08	0.081 29	0.258 50
H82	−0.032 98	0.933 79	0.257 59	0.085 20
H83	0.102 09	0.963 60	0.155 86	0.085 20
H84	0.312 64	0.839 94	0.072 06	0.085 20
H85	0.534 06	0.597 50	0.029 30	0.085 20
H86	0.606 24	0.326 64	0.085 04	0.085 20
H87	0.458 43	0.298 16	0.185 00	0.085 20
H88	0.191 13	0.407 29	0.312 14	0.085 20
H89	−0.156 52	0.403 78	0.393 73	0.040 30

O44–H88···O43 *S*1,1(6) hydrogen bond in the xinafoate anion. The hydroxyl group O9 acts as an acceptor in two C–H···O hydrogen bonds. Although weak, these C–H donor hydrogen bonds probably contribute significantly to the crystal energy. These hydrogen bonds result in complex chains along the *b*-axis.

The volume enclosed by the Hirshfeld surface (Figure 6; Hirshfeld, 1977; McKinnon *et al.*, 2004; Spackman and Jayatilaka, 2009; Wolff *et al.*, 2012) is 809.50 Å^3, 99.4% of

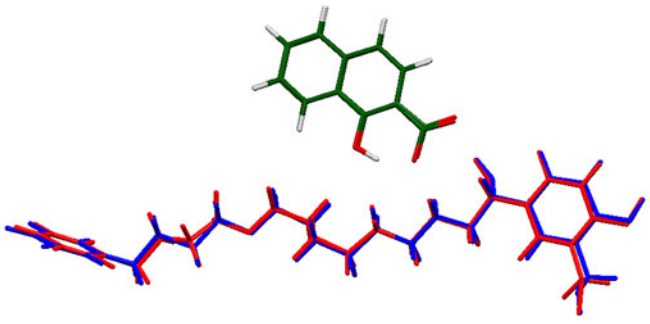

Figure 3. (Colour online) Comparison of the refined and optimized structures of salmeterol xinafoate. The Rietveld-refined structure is in red, and the DFT-optimized structure is in blue.

https://doi.org/10.1017/S0885715615000743 Published online by Cambridge University Press

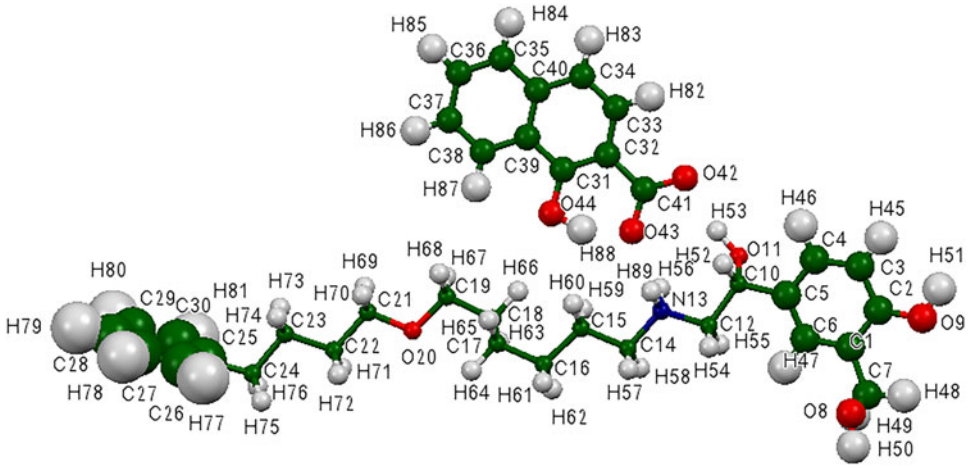

Figure 4. (Colour online) The molecular structure of salmeterol xinafoate, with the atom numbering. The atoms are represented by 50% probability spheroids.

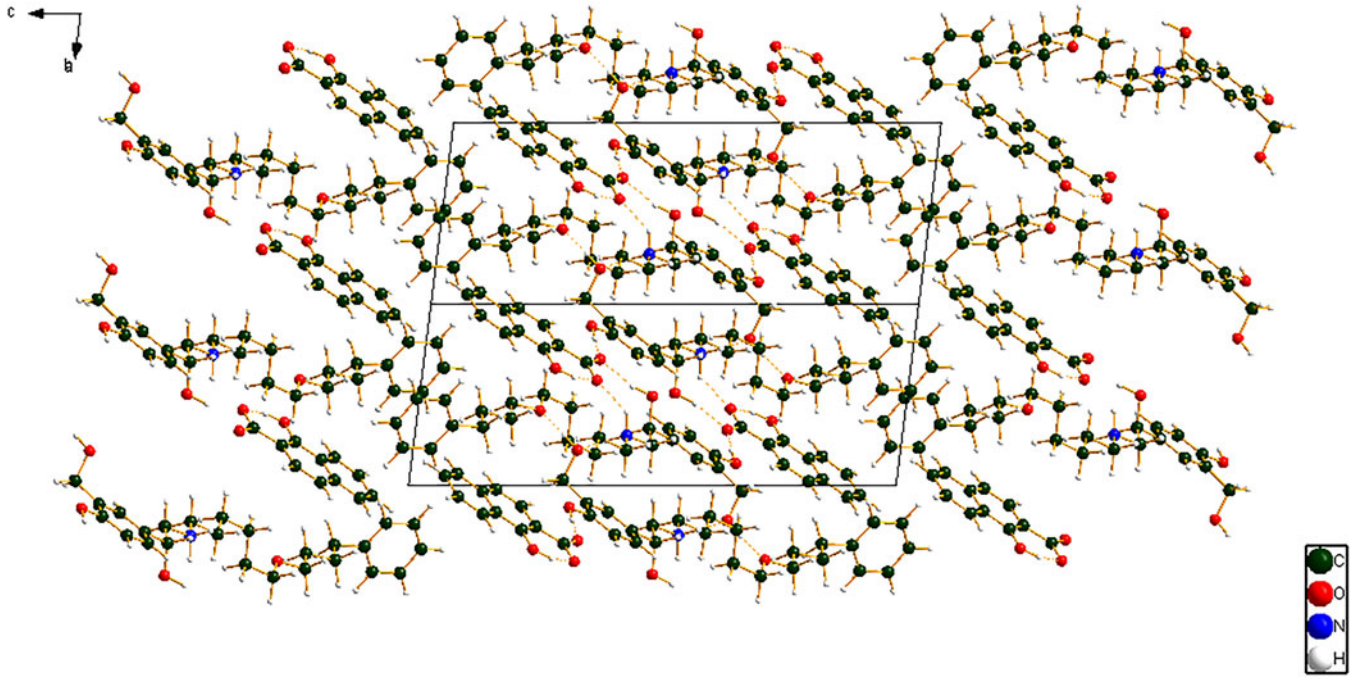

Figure 5. (Colour online) The crystal structure of salmeterol xinafoate, viewed down the [−110]-axis. The hydrogen bonds are shown as dashed lines.

half the unit-cell volume. The molecules are thus not tightly packed. The only significant close contacts (red in Figure 6) involve the hydrogen bonds.

The Bravais–Friedel–Donnay–Harker (Bravais, 1866; Friedel, 1907; Donnay and Harker, 1937) morphology suggests that we might expect platy morphology for salmeterol xinafoate, with {001} as the principal faces. A fourth-order spherical harmonic-preferred orientation model was included in the refinement; the texture index was 1.076, indicating that preferred orientation was significant in this rotated

TABLE III. Hydrogen bonds in the DFT-optimized crystal structure of salmeterol xinafoate.

D–*H*···*A*	*D*–*H* (Å)	*H*···*A* (Å)	*D*···*A* (Å)	*D*–*H*···*A* (°)	Overlap (*e*)
N13–H89···O8	1.047	1.750	2.779	166.9	0.076
N13–H56···O43	1.035	1.907	2.746	135.8	0.041
O44–H88···O43	1.018	1.515	2.468	153.6	0.084
O9–H51···O42	0.997	1.666	2.662	178.8	0.067
O8–H50···O20	0.984	1.740	2.722	175.4	0.060
O11–H53···O42	0.986	1.837	2.804	166.2	0.055
C33–H82···O9	1.083	2.385	3.417	158.8	0.017
C7–H48···O9	1.093	2.427	2.849	101.2	0.012

https://doi.org/10.1017/S0885715615000743 Published online by Cambridge University Press

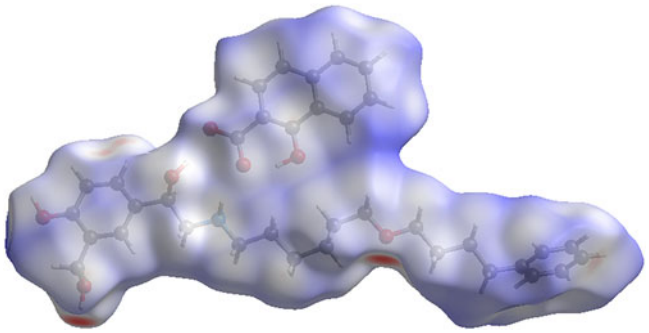

Figure 6. (Colour online) The Hirshfeld surface of salmeterol xinafoate. Intermolecular contacts longer than the sums of the van der Waals radii are colored blue, and contacts shorter than the sums of the radii are colored red. Contacts equal to the sums of radii are white.

capillary specimen. The powder pattern of salmeterol xinafoate has been submitted to ICDD for inclusion in the PDF as entry 00-065-1430.

SUPPLEMENTARY MATERIALS AND METHODS

To view supplementary material for this article, please visit http://dx.doi.org/10.1017/S0885715615000743

ACKNOWLEDGEMENTS

Use of the Advanced Photon Source at Argonne National Laboratory was supported by the U.S. Department of Energy, Office of Science, Office of Basic Energy Sciences, under Contract No. DE-AC02-06CH11357. This work was partially supported by the International Centre for Diffraction Data. We thank Lynn Ribaud for his assistance in data collection.

Accelrys (**2013**). *Materials Studio 7.0* (Accelrys Software Inc., San Diego, CA).

Allen, F. H. (**2002**). "The Cambridge Structural Database: a quarter of a million crystal structures and rising," Acta Crystallogr., B: Struct. Sci. **58**, 380–388.

Altomare, A., Cuocci, C., Giacovazzo, C., Moliterni, A., Rizzi, R., Corriero, N., and Falcicchio, A. (**2013**). "EXPO2013: a kit of tools for phasing crystal structures from powder data", J. Appl. Crystallogr. **46**, 1231–1235.

Beach, S., Latham, D., Sidgwick, C., Hanna, M., and York, P. (**1999**). "Control of the physical form of salmeterol xinafoate," Org. Proc. Res. Dev. **3**, 370–376.

Bernstein, J., Davis, R. E., Shimoni, L., and Chang, N. L. (**1995**). "Patterns in hydrogen bonding: functionality and graph set analysis in crystals," Angew. Chem. Int. Ed. Engl. **34**(15), 1555–1573.

Bravais, A. (**1866**). *Etudes Cristallographiques* (Gauthier Villars, Paris).

Bruno, I. J., Cole, J. C., Kessler, M., Luo, J., Motherwell, W. D. S., Purkis, L. H., Smith, B. R., Taylor, R., Cooper, R. I., Harris, S. E., and Orpen, A. G. (**2004**). "Retrieval of crystallographically-derived molecular geometry information," J. Chem. Inf. Sci. **44**, 2133–2144.

David, W. I. F., Shankland, K., van de Streek, J., Pidcock, E., Motherwell, W. D. S., and Cole, J. C. (**2006**). "DASH: a program for crystal structure determination from powder diffraction data," J. Appl. Crystallogr. **39**, 910–915.

Donnay, J. D. H. and Harker, D. (**1937**). "A new law of crystal morphology extending the law of Bravais," Am.. Mineral. **22**, 446–467.

Dovesi, R., Saunders, V. R., Roetti, C., Orlando, R., Zicovich-Wilson, C. M., Pascale, F., Civalleri, B., Doll, K., Harrison, N. M., Bush, I. J., D-Arco, Ph., Llunell, M., Causà, M., and Noël, Y. (**2014**). *CRYSTAL14 User's Manual*. University of Torino; http://www.crystal.unito.it.

Etter, M. C. (**1990**). "Encoding and decoding hydrogen-bond patterns of organic compounds," Acc. Chem. Res. **23**(4), 120–126.

Favre-Nicolin, V. and Černý, R. (**2002**). "FOX, Free Objects for crystallography: a modular approach to ab initio structure determination from powder diffraction," J. Appl. Crystallogr. **35**, 734–743.

Finger, L. W., Cox, D. E., and Jephcoat, A. P. (**1994**). "A correction for powder diffraction peak asymmetry due to axial divergence," J. Appl. Crystallogr. **27**(6), 892–900.

Friedel, G. (**1907**). "Etudes sur la loi de Bravais," Bull. Soc. Fr. Mineral. **30**, 326–455.

Gatti, C., Saunders, V. R., and Roetti, C. (**1994**). "Crystal-field effects on the topological properties of the electron-density in molecular crystals – the case of urea," J. Chem. Phys. **101**, 10686–10696.

Hirshfeld, F. L. (**1977**). "Bonded-atom fragments for describing molecular charge densities," Theor. Chem. Acta **44**, 129–138.

ICDD (**2014**), PDF-4+ 2014 (Database), edited by Dr. Soorya Kabekkodu International Centre for Diffraction Data, Newtown Square, PA, USA.

Larson, A. C. and Von Dreele, R. B. (**2004**). *General Structure Analysis System (GSAS)*, (Report LAUR 86-784). Los Alamos, New Mexico: Los Alamos National Laboratory.

Lee, P. L., Shu, D., Ramanathan, M., Preissner, C., Wang, J., Beno, M. A., Von Dreele, R. B., Ribaud, L., Kurtz, C., Antao, S. M., Jiao, X., and Toby, B. H. (**2008**). "A twelve-analyzer detector system for high-resolution powder diffraction," J. Synchrotron Radiat. **15**(5), 427–432.

Macrae, C. F., Bruno, I. J., Chisholm, J. A., Edington, P. R., McCabe, P., Pidcock, E., Rodriguez-Monge, L., Taylor, R., van de Streek, J., and Wood, P. A. (**2008**). "Mercury CSD 2.0 – new features for the visualization and investigation of crystal structures," J. Appl. Crystallogr. **41**, 466–470.

McKinnon, J. J., Spackman, M. A., and Mitchell, A. S. (**2004**). "Novel tools for visualizing and exploring intermolecular interactions in molecular crystals," Acta Crystallogr. B **60**, 627–668.

MDI (**2014**). *Jade 9.5* (Materials Data. Inc., Livermore, CA).

O'Boyle, N., Banck, M., James, C. A., Morley, C., Vandermeersch, T., and Hutchison, G. R. (**2011**). "Open Babel: an open chemical toolbox," J. Chem. Inf. **3**, 33. DOI: 10.1186/1758-2946-3-33.

Shields, G. P., Raithby, P. R., Allen, F. H., and Motherwell, W. S. (**2000**). "The assignment and validation of metal oxidation states in the Cambridge Structural Database," Acta Crystallogr. B **56**(3), 455–465.

Spackman, M. A. and Jayatilaka, D. (**2009**). "Hirshfeld surface analysis," Cryst. Eng. Commun. **11**, 19–32.

Stephens, P. W. (**1999**). "Phenomenological model of anisotropic peak broadening in powder diffraction," J. Appl. Crystallogr. **32**, 281–289.

Sykes, R. A., McCabe, P., Allen, F. H., Battle, G. M., Bruno, I. J., and Wood, P. A. (**2011**). "New software for statistical analysis of Cambridge Structural Database data," J. Appl. Crystallogr. **44**, 882–886.

Thompson, P., Cox, D. E., and Hastings, J. B. (**1987**). "Rietveld refinement of Debye-Scherrer synchrotron X-ray data from Al_2O_3," J. Appl. Crystallogr. **20**(2), 79–83.

Toby, B. H. (**2001**). "EXPGUI, a graphical user interface for GSAS," J. Appl. Crystallogr. **34**, 210–213.

Tong, H. H. Y., Shekunov, B. Yu., York, P., and Chow, A. H. L. (**2001**). "Characterization of two polymorphs of salmeterol xinafoate crystallized from supercritical fluids," Pharm. Res. **18**, 852–858.

van de Streek, J. and Neumann, M. A. (**2014**). "Validation of molecular crystal structures from powder diffraction data with dispersion-corrected density functional theory (DFT-D)," Acta Crystallogr. B **70**(6), 1020–1032.

Wang, J., Toby, B. H., Lee, P. L., Ribaud, L., Antao, S. M., Kurtz, C., Ramanathan, M., Von Dreele, R. B., and Beno, M. A. (**2008**). "A dedicated powder diffraction beamline at the Advanced Photon Source: commissioning and early operational results," Rev. Sci. Instrum. **79**, 085105.

Wavefunction, Inc. (**2013**). Spartan '14 Version 1.1.0 (Wavefunction Inc.), 18401 Von Karman Ave., Suite 370, Irvine CA 92612.

Wolff, S. K., Grimwood, D. J., McKinnon, M. J., Turner, M. J., Jayatilaka, D., and Spackman, M. A. (**2012**). CrystalExplorer Version 3.1 (University of Western Australia).